Supersensitive, Ultrafast, and Broad-Band Light-Harvesting Scheme Employing Carbon Nanotube/TiO_2 Core–Shell Nanowire Geometry

Chia-Yang Hsu,[†,§] Der-Hsien Lien,[†,§] Sheng-Yi Lu,[‡] Cheng-Ying Chen,[†] Chen-Fang Kang,[†] Yu-Lun Chueh,[‡] Wen-Kuang Hsu,[‡] and Jr-Hau He[†,*]

[†]Department of Electrical Engineering & Institute of Photonics and Optoelectronics, National Taiwan University, Taipei 10617, Taiwan and [‡]Department of Materials Science and Engineering, National Tsing Hua University, Hsinchu 30013, Taiwan. [§]These authors contributed equally to this work.

ABSTRACT

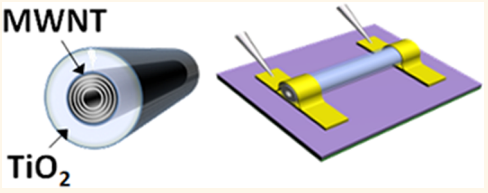

We demonstrate a novel, feasible strategy for practical application of one-dimensional photodetectors by integrating a carbon nanotube and TiO_2 in a core–shell fashion for breaking the compromise between the photogain and the response/recovery speed. Radial Schottky barriers between carbon nanotube cores and TiO_2 shells and surface states at TiO_2 shell surface regulate electron transport and also facilitate the separation of photogenerated electrons and holes, leading to ultrahigh photogain ($G = 1.4 \times 10^4$) and the ultrashort response/recovery times (4.3/10.2 ms). Additionally, radial Schottky junction and defect band absorption broaden the detection range (UV–visible). The concept using metallic core oxide–shell geometry with radial Schottky barriers holds potential to pave a new way to realize nanostructured photodetectors for practical use.

KEYWORDS: core–shell · TiO_2 · carbon nanotube · photodetector · photoresponse time

One-dimensional metal oxide nanostructures as photodetectors (PDs) exhibiting high photoconductive gain have stimulated much interest due to the pronounced surface effects (*i.e.*, oxygen adsorption/desorption) originating from the high surface-to-volume ratio.[1,2] The photogain as high as 10^8 has been reported using ZnO nanowires (NWs).[3,4] In an attempt to achieve high-performance photodetection, most studies have focused on boosting the photosensitivity.[5,6] Although the high photogain is achieved, these surface effects act as a double-edged sword that prolongs the response/recovery time due to slow oxygen adsorption/desorption processes, thus hindering practical applications of metal oxide nanostrucutures in PDs. Several approaches to break this compromise for enhancing the responsibility as well as reducing the response/recovery times have been reported, including an introduction of Schottky junction,[7] the modification of surfaces,[5,6] the reduction of nanowire sizes,[8] and the fabrication of network structures.[9] However, to realize the nanostructured metal oxide PDs in practical use, further improvement toward higher gain and faster response is urgently demanded.

The heterojunction between two different nanomaterials in a variety of nanostructures, such as core–shell NWs,[10–13] segmented NWs,[14,15] and core–shell quantum dots,[16] has shown great potential for the application in solar cells, biosensors, photodetection, and piezoelectric nanogenerators.[13,17–21] For example, the semiconducting core–shell NW geometry can enhance the efficiency of charge collection by shortening the paths traveled by minority carriers and therefore can promote energy-harvesting properties.[17–20] The NWs with semiconducting cores encapsulated by dielectric shells not only provide excellent surface passivation but also offer excellent light-harvesting characteristics, such as broad-band working ranges, omnidirectionality, and polarization insensitivity since the dielectric shell is capable of creating a smooth gradient of refractive index profiles.[21]

In this study, we used metallic multiwalled carbon nanotubes (MWNTs) as inner cores and semiconducting TiO_2 as outer shells to create 1D core–shell nanostructures for supersensitive, ultrafast, and

* Address correspondence to jhhe@cc.ee.ntu.edu.tw.

Received for review March 15, 2012 and accepted July 31, 2012.

Published online August 15, 2012
10.1021/nn3011625

broad-band photodetection. Among metal oxide candidates, TiO_2, a wide band gap material (3.2 eV for anatase), is promising for the photodetection with a fast response speed and a high gain and thus could efficiently serve as a photon adsorption layer in this unique structure by enhancing charge separation promoted by the surface states.[22] On the other hand, MWNT cores provide radial Schottky barriers to TiO_2 shells to regulate electron transport and also facilitates the separation of photogenerated electrons and holes. Accordingly, the photogain up to 1.4×10^4 can be achieved, and the response/recovery times are promoted to 4.3/10.2 ms. Broad-band detection is also accomplished by the additional absorption from MWNTs possibly due to the radial Schottky junction between MWNTs and TiO_2 shells and the defect band absorption. The concept of the core–shell nanowire geometry reported herein explores a new pathway toward ultrafast, supersensitive, and broad-band photodetection.

RESULTS AND DISCUSSION

Aligned MWNTs were synthesized at 1400 °C using ferrocene-dissolved xylene (1:50, 100 mL) as the carbon source.[23,24] Then, atomic layer deposition (ALD) was employed to deposit TiO_2 on the MWNTs,[24] as shown in the Supporting Information. With precise control of TiO_2 growth, a 5 nm thick TiO_2 layer was deposited on MWNTs to ensure sufficient light absorption. Since the photon-to-electron conversion efficiency is highly dependent on the crystallinity of the active layer (*i.e.*, TiO_2),[1,25] an annealing process was performed at 450 °C in Ar for 2 h. Moreover, according to the previous reports,[26,27] 5 nm thickness could absorb about 10–15% of light from visible to UV region. Since the incident light will penetrate the TiO_2 layer twice due to the core–shell geometry, we could expect that the light absorption will be over 20%, which is sufficient for photoexcitation.

A single TiO_2–MWNT core–shell PD was fabricated with the assistance of electron-beam lithography (EBL), as shown in a scanning electron microscopy (SEM) image and the schematic in Figure 1a (see Supporting Information for fabrication details). The core–shell NWs were dispersed in isopropyl alcohol and then transferred onto the SiO_2/Si substrate by dropping NWs from a pipet. To contact a core–shell single NW, the electrode patterns were defined by SEM and then followed by Ti/Au (30 nm/70 nm) electrode fabrication *via* the EBL process. Before testing the performance of the MWNT/TiO_2 core–shell NW PD, the material properties were characterized. Figure 1b shows the analyses of X-ray diffraction (XRD) of core–shell NWs before and after the annealing. Before annealing, no significant feature was observed, indicating the poor crystallinity of the TiO_2 layer, while after the heat treatment, evident peaks at 24.5 and 37° were observed,

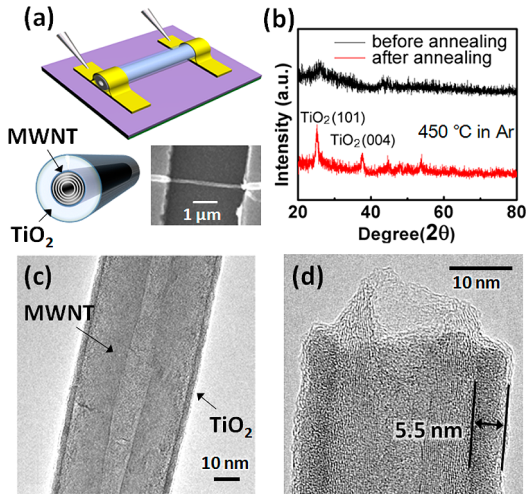

Figure 1. (a) Schematics of the core–shell nanostructure and the corresponding PD. Inset shows the SEM image of the device. (b) XRD spectra of the core–shell NW before and after the annealing process. (c) TEM image of a core–shell NW. (d) High-resolution TEM image of a core–shell NW at the end.

corresponding to (101) and (004) planes of the anatase TiO_2, respectively. Transmission electron microscopy (TEM) further displays the features of the core–shell nanostructures. A uniformly coated TiO_2 shell is observed in Figure 1c, where the TiO_2 is darker because of heavier molecular weight, and the inner structures with stripe fringes are the walls of the MWNT. Further analysis shows that the MWNTs have diameters ranging from 20 to 60 nm, and the thickness of TiO_2 shells is ~5 nm (Figure 1d), consistent with the ALD fabrication parameters.

The electrical measurements were carried out at room temperature using a semiconductor parameter analyzer (Keithley Instruments 4200), and the photoresponse was characterized under air mass 1.5 global (AM 1.5G) illumination (1000 W/m^2) and a halogen lamp coupled to a monochromator. Before verifying the performance of the MWNT/TiO_2 core–shell NW PD, the role of the core MWNT was first examined. A single MWNT device without TiO_2 shells, serving as a control, was made *via* the same process, and its *IV* characteristic is shown in Figure 2a. The quasi-linear *IV* curve, representing the most classic electrical behavior of MWNT devices, reveals the fact that the MWNT is metallic. As for the photoresponse of the MWNT device, the *IV* curve under AM 1.5G illumination remains the same as that in the dark, indicating that the metallic MWNT is insensitive to light.[28] The photoresponse of the MWNT/TiO_2 core–shell NW is shown in Figure 2b. As compared to the pure MWNT device, the MWNT/TiO_2 core–shell NW PD exhibits an apparent response to AM 1.5G light, demonstrating the role of TiO_2 in the photocurrent generation. Note that the contacts between the Ti electrodes with work function φ_m of ~4.3 eV and the TiO_2 shell with electron affinity of ~4.3 eV are ohmic.[29]

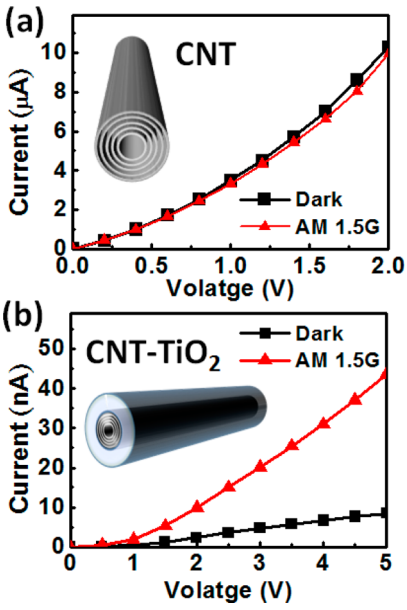

Figure 2. (a) *IV* characteristics of the MWNT device in the dark and upon AM 1.5G illumination. (b) *IV* characteristics of the TiO_2-coated MWNT PD in the dark and upon AM 1.5G illumination.

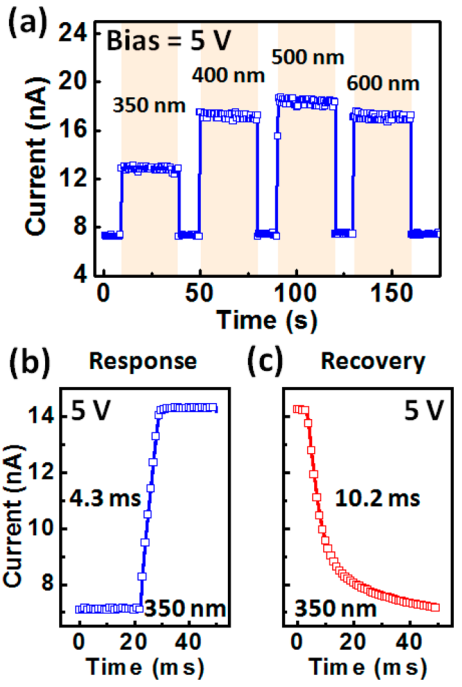

Figure 3. (a) Time-resolved photocurrents of the TiO_2-coated device under various wavelengths illumination at 5 V. (b) Highlights of the response speed under 350 nm illumination at 5 V. (c) Highlights of the recovery speed under 350 nm illumination at 5 V.

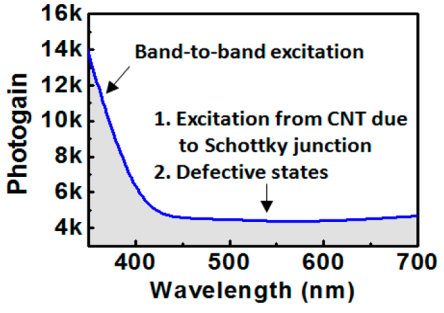

Figure 4. Photogain of the core–shell NW PD as a function of wavelengths. Three mechanisms are depicted on the graph, which can be attributed to different absorption ranges.

To highlight the ultrafast response of the devices, the time-resolved measurements were performed at a fixed bias of 5 V. As shown in Figure 3a, a fully reversible response was acquired; the current abruptly increased and then decreased to its initial value as the light was on and off, respectively. The amplification ratios of photocurrents range from 160 to 250%, depending on the optical wavelengths and the incident power. Note that the power density of a halogen lamp used here is varied with the wavelength. For quantitative analysis, the wavelength-dependent photogain will be carried out later. To probe the temporal response in a high resolution, we set up a data acquisition system (DAQ; DAQ-2214, ADLINK) operated with a resolution as low as 10 μs. One can see that a short response/recovery time regardless of the wavelength is obtained, as shown in an example in Figure 3b,c at an incident wavelength of 350 nm. Here the data are partially skipped in order to more clearly reveal the difference between response and recovery speed; the interval of each data point presented in the figures is 1 ms. The response and the recovery times can be used to evaluate the speed of response and recovery processes, which are defined as the time needed to rise to $(1 - 1/e)$ of the dark current and recover to $1/e$ of the maximum photocurrent, respectively.[30] Accordingly, 4.3 ms of the response and 10.2 ms of the recovery times can be obtained. To the best of our knowledge, this is the fastest response/recovery speed reported for any TiO_2-based PD to date.[22]

The importance of metallic core–semiconducting shell geometry in the photodetection can also be understood by the spectral photoresponse measurements, as presented in Figure 4. The photogain is calculated by $G = (\Delta I_{ph}/q)/(P/h\nu)$, where ΔI_{ph} is the difference between measured photocurrent and dark current, q is the electron charge, P is the power of incident light absorbed by the device, and $h\nu$ is the photon energy. To obtain the power of incident light absorbed by the device, the light absorption area of the device is estimated according to the SEM and the TEM images of the device, where the length and the width of the nanostructure is 3.2 μm and 65 nm, respectively. Note that the incident power is dependent on the incident wavelength and thus is normalized as computing the photoconductive gain (see Supporting Information). The photogain has a ramp at UV region because the TiO_2, a wide band gap semiconductor (3.2 eV), has remarkable UV absorption property. Interestingly, the

photoresponse in the regime higher than 400 nm is also obvious and could be attributed to two mechanisms associated with the structure effects: (i) Because of the radial Schottky junction between the MWNT core and the TiO_2 shell, the device possesses an exclusive light absorption pathway; that is, the photocarriers are excited from metallic MWNTs over the Schottky barrier.[31] Therefore, in addition to band-to-band excitation in the TiO_2 shell, the electrons could be excited from the metallic MWNT to the conduction band of the TiO_2 shell, resulting in additional broad-band absorption. To undergo this process, the incident photon energy must be higher than the blocking barrier (φ_b)[32] that originates from the radial Schottky contact between the metallic MWNT core (work function φ_m = 4.9 eV)[33] and the semiconducting n-type TiO_2 shell (electron affinity χ = 4.3 eV).[34−36] According to the equation $\varphi_b = \chi - \varphi_m$, the ideal φ_b between MWNTs and TiO_2 = 0.6 eV is low, thus the absorption spectrum can be widely extended toward long wavelength region. (ii) Another possible factor for observed broad-band absorption is the presence of sub-band gap due to the defects in TiO_2 or the interfacial defects at the MWNT−TiO_2 junction.[37−42] Those defect-induced states can broaden the absorption spectra and have been widely demonstrated in other heterojunction systems.[43] Note that, on the basis of current data, we cannot verify which mechanism dominates because the resultant effect might be a combination of both.

In comparison to other TiO_2-based PDs with high photogains reported elsewhere, 1.4×10^4 of the maximum photogain of the core−shell NW in the UV region (Figure 4) is about 4 orders of magnitude higher than those of TiO_2 nanotube arrays (~52).[44] For metal oxide NWs, it is known that the process of oxygen adsorption [$O_{2(g)} + e^- \rightarrow O_2^-{}_{(ad)}$] and desorption [$O_2^-{}_{(ad)} + h^+ \rightarrow O_{2(g)}$] on the NW surfaces dominates the photocarrier transport and the photoresponse behavior.[3,4] The origin of the photogain of metal oxide nanostructures is closely connected to the long lifetime of the photogenerated electrons, resulting from the hole-trapping effect activated by the oxygen desorption at the surfaces, which significantly reduces the recombination rate of electron−hole pairs. Accordingly, the photogain can also be expressed as $G = \tau/\tau_t$, where τ is the carrier lifetime (recovery time) and τ_t is the transit time between two electrodes.[45] Since τ_t is a function only related to experimental parameters and material mobility, this equation implies a trade-off between the photogain and the response speed ($\propto 1/\tau$). This can be confirmed by the fact that most of the PDs with a high photogain exhibit a slow response speed ranging from tens of seconds to several hours.[1,3,7] A major breakthrough in this study is that the MWNT−TiO_2 core−shell NW not only retains the high gain but also possesses high response speed, diminishing the compromise between photogain and response speed.

Possessing ultrahigh photogains and ultrashort response/recovery times at the same time could be attributed to the unique core−shell geometry of the MWNT−TiO_2 NWs. Full depletion of ~5 nm thick TiO_2 is formed due to (i) the space charge layer formed at the surface of TiO_2 shells and (ii) the radial Schottky barrier between MWNT cores and TiO_2 shells, which can be confirmed by the very low dark current of the core−shell NW device, as shown in Figure 2b. Under illumination, the processes of oxygen desorption/adsorption at the surface and the radial Schottky barrier modulation effectively activate a reversible regulation of depletion width and height, leading to a great enhancement of the photogain. The rapid photocurrent response and recovery are related to the fact stated as follows. Under illumination, the strong local electric field in the TiO_2 core assisted by the oxygen desorption/adsorption and the radial Schottky junctions will quickly separate the photon-generated electrons and holes, giving rise to a rapid response speed, as shown in Figure 3b. Under illumination, the increase of the photon-generated carrier density leads to a reduction of the barrier height and a narrowing of the barrier width, enabling the access of the photoinduced low-resistive conducting path within the depleted TiO_2 and thus increasing the conductivity of the core−shell NW. It has been known that the process of the light-induced Schottky barrier modulation is rather fast.[9] Accordingly, the response/recovery time can be dramatically reduced. We note that, in previous studies, two types of Schottky contacts pertaining to NW PDs have been demonstrated, including the Schottky contact between planar metal electrodes and NWs[7] and the NW-to-NW contacts within NW networks,[9] both of which have shown the enhancement to response speed. Moreover, we envision that the photoresponse of our devices can be further improved after optimizing the thickness of the TiO_2 layer for maximizing the light absorption and the depleted region. Moreover, using the aligned array of CNT/TiO_2 core−shell NWs that capitalizes on a strong light-trapping effect at a variety of wavelengths and angles of incidence might significantly increase the amount of photons absorbed at the radial junction regions due to it subwavelength structure.[46,47] In addition, Cao *et al.* reported the use of the 1D nanostructure resonance property by tuning the radius of nanowires so that the light absorption can be enhanced at resonance regions, referred to as the leaky mode resonance enhancement.[48,49] Implementing the above-mentioned concepts into CNT−TiO_2 core−shell PDs might be an important concern for applying it to practical applications in the future.

In summary, we break the compromise between photogains and response/recovery times of nanowire PDs using metallic MWNT−semiconducting TiO_2

core−shell nanowires. MWNT−TiO_2 NW PDs exhibit high photogains of up to 1.4×10^4 and short response/recovery times of 4.3/10.2 ms with the broad-band detection. The ultrasensitive and ultrafast photodetection achieved in MWNT−TiO_2 core−shell NWs is due to enhanced charge separation promoted by the surface states and the radial Schottky barrier between MWNT cores and TiO_2 shells. The broad-band detection results from additional absorption from MWNTs due to Schottky junction and defect band absorption. The resultant performance is essentially useful for fabricating photovoltaic and photodetection devices based on core−shell nanowire heterojunctions.

Conflict of Interest: The authors declare no competing financial interest.

Acknowledgment. This work was supported by National Science Council of Taiwan (99-2622-E-002-019-CC3, 99-2112-M-002-024-MY3, and 99-2120-M-007-011).

Supporting Information Available: Synthesis and device fabrication of MWNT arrays and MWNT−TiO_2 core−shell structures. This material is available free of charge *via* the Internet at http://pubs.acs.org.

REFERENCES AND NOTES

1. Chen, C. Y.; Chen, M. W.; Ke, J. J.; Lin, C. A.; Retamal, J. R. D.; He, J. H. Surface Effect on Optical and Electrical Properties of ZnO Nanostructure. *Pure Appl. Chem.* **2008**, *82*, 2055–2073.
2. Gao, P.; Wang, Z. Z.; Liu, K. H.; Xu, Z.; Wang, W. L.; Bai, X. D.; Wang, E. G. Photoconducting Response on Bending of Individual ZnO Nanowires. *J. Mater. Chem.* **2009**, *19*, 1002–1005.
3. Soci, C.; Zhang, A.; Xiang, B.; Dayeh, S. A.; Aplin, D. P. R.; Park, J.; Bao, X. Y.; Lo, Y. H.; Wang, D. ZnO Nanowire UV Photodetectors with High Internal Gain. *Nano Lett.* **2007**, *7*, 1003–1009.
4. He, J. H.; Chang, P. H.; Chen, C. Y.; Tsai, K. T. Electrical and Optoelectronic Characterization of ZnO Nanowire Contacted by Focused-Ion-Beam-Deposited Pt. *Nanotechnology* **2009**, *20*, 135701.
5. Chen, M. W.; Chen, C. Y.; Lien, D. H.; Ding, Y.; He, J. H. Photoconductive Enhancement of Single ZnO Nanowire through Localized Schottky Effects. *Opt. Express* **2010**, *18*, 14836–14841.
6. Lao, C. S.; Park, M. C.; Kuang, Q.; Deng, Y.; Sood, A. K.; Polla, D. L.; Wang, Z. L. Giant Enhancement in UV Response of ZnO Nanobelts by Polymer Surface-Functionalization. *J. Am. Chem. Soc.* **2007**, *129*, 12096–12097.
7. Zhou, J.; Gu, Y.; Hu, Y.; Mai, W.; Yeh, P. H.; Bao, G.; Sood, A. K.; Polla, D. L.; Wang, Z. L. Gigantic Enhancement in Response and Reset Time of ZnO UV Nanosensor by Utilizing Schottky Contact and Surface Functionalization. *Appl. Phys. Lett.* **2009**, *94*, 191103.
8. Chen, M. W.; Retamal, J. R. D.; Chen, C. Y.; He, J. H. Photocarrier Relaxation Behavior of a Single ZnO Nanowire UV Photodetector: Effect of Surface Band Bending. *IEEE Electron Device Lett.* **2012**, *33*, 411–413.
9. Chen, C. Y.; Chen, M. W.; Hsu, C. Y.; Lien, D. H.; Chen, M. J.; He, J. H. Enhanced Recovery Speed of Nanostructured ZnO Photodetectors Using Nanobelt Networks. *IEEE J. Sel. Top. Quantum Electron.* **2012**, DOI:10.1109/JSTQE.2012.2200031.
10. Chueh, Y. L.; Hsieh, C. H.; Chang, M. T.; Chou, L. J.; Lao, C. S.; Song, J. H.; Gan, J. Y.; Wang, Z. L. RuO_2 Nanowires and RuO_2/TiO_2 Core/Shell Nanowires: From Synthesis to Mechanical, Optical, Electrical, and Photoconductive Properties. *Adv. Mater.* **2007**, *19*, 143–149.
11. Goldberger, J.; Hochbaum, A. I.; Fan, R.; Yang, P. Silicon Vertically Integrated Nanowire Field Effect Transistors. *Nano Lett.* **2006**, *6*, 973–977.
12. Mieszawska, A. J.; Jalilian, R.; Sumanasekera, G. U.; Zamborini, F. P. The Synthesis and Fabrication of One-Dimensional Nanoscale Heterojunctions. *Small* **2007**, *3*, 722–756.
13. Hu, C. J.; Lin, Y. H.; Tang, C. W.; Tsai, M. Y.; Hsu, W. K.; Kuo, H. F. ZnO-Coated Carbon Nanotubes: Flexible Piezoelectric Generators. *Adv. Mater.* **2011**, *23*, 2941–2945.
14. Gudiksen, M. S.; Lauhon, L. J.; Wang, J.; Smith, D. C.; Lieber, C. M. Growth of Nanowire Superlattice Structures for Nanoscale Photonics and Electronics. *Nature* **2002**, *415*, 617–620.
15. Liu, J.; Li, X.; Dai, L. Water-Assisted Growth of Aligned Carbon Nanotube-ZnO Heterojunction Arrays. *Adv. Mater.* **2006**, *18*, 1740–1744.
16. Medintz, I. L.; Uyeda, H. T.; Goldman, E. R.; Mattoussi, H. Quantum Dot Bioconjugates for Imaging, Labelling and Sensing. *Nat. Mater.* **2005**, *4*, 435–446.
17. Tian, B.; Zheng, X.; Kempa, T. J.; Fang, Y.; Yu, N.; Yu, G.; Huang, J.; Lieber, C. M. Coaxial Silicon Nanowires as Solar Cells and Nanoelectronic Power Sources. *Nature* **2007**, *449*, 885–889.
18. Kayes, B. M.; Atwater, H. A.; Lewis, N. S. Comparison of the Device Physics Principles of Planar and Radial P−N Junction Nanorod Solar Cells. *J. Appl. Phys.* **2005**, *97*, 114302.
19. Tang, J.; Huo, Z.; Brittman, S.; Gao, H.; Yang, P. Solution-Processed Core−Shell Nanowires for Efficient Photovoltaic Cells. *Nat. Nanotechnol.* **2011**, *6*, 568–572.
20. Tsai, S. H.; Chang, H. C.; Wang, H. H.; Chen, S. Y.; Lin, C. A.; Chen, S. A.; Chueh, Y. L.; He, J. H. Significant Efficiency Enhancement of Hybrid Solar Cells Using Core−Shell Nanowire Geometry for Energy Harvesting. *ACS Nano* **2011**, *5*, 9501–9510.
21. Lai, K. Y.; Chang, H. C.; Dai, Y. A.; He, J. H. Photon Management with Core−Shell Nanowire Structures. *Opt. Express* **2012**, *20*, A255–A264.
22. Zhai, T.; Li, L.; Wang, X.; Fang, X.; Bando, Y.; Golberg, D. Recent Developments in One-Dimensional Inorganic Nanostructures for Photodetectors. *Adv. Funct. Mater.* **2010**, *20*, 4233–4248.
23. Andrews, R.; Jacques, D.; Rao, A. M.; Derbyshire, F.; Qian, D.; Fan, X.; Dickey, E. C.; Chen, J. Continuous Production of Aligned Carbon Nanotubes: A Step Closer to Commercial Realization. *Chem. Phys. Lett.* **1999**, *303*, 467–474.
24. Lu, S. Y.; Tang, C. W.; Lin, Y. H.; Kuo, H. F.; Lai, Y. C.; Tsai, M. Y.; Ouyang, H.; Hsu, W. K. TiO_2-Coated Carbon Nanotubes: A Redshift Enhanced Photocatalysis at Visible Light. *Appl. Phys. Lett.* **2010**, *96*, 231915.
25. Li, L.; Lee, P. S.; Yan, C.; Zhai, T.; Fang, X.; Liao, M.; Koide, Y.; Bando, Y.; Golberg, D. Ultrahigh-Performance Solar-Blind Photodetectors Based on Individual Single-Crystalline $In_2Ge_2O_7$ Nanobelts. *Adv. Mater.* **2010**, *22*, 5145–5149.
26. Halary-Wagner, E.; Wagner, F.; Hoffmann, P. Titanium Dioxide Thin-Film Deposition on Polymer Substrate by Light Induced Chemical Vapor Deposition. *J. Electrochem. Soc.* **2004**, *151*, C571–C576.
27. Kim, H; Auyeung, R. C. Y.; Ollinger, M.; Kushto, G. P.; Kafafi, Z. H.; Piqué, A. Laser-Sintered Mesoporous TiO_2 Electrodes for Dye-Sensitized Solar Cells. *Appl. Phys. A: Mater. Sci. Process.* **2006**, *83*, 73–76.
28. Freitag, M.; Martin, Y.; Misewich, J. A.; Martel, R.; Avouris, P. Photoconductivity of Single Carbon Nanotubes. *Nano Lett.* **2003**, *3*, 1067–1071.
29. Fuke, N.; Fukui, A.; Islam, A.; Komiya, R.; Yamanaka, R.; Harima, H.; Han, L. Influence of TiO_2/Electrode Interface on Electron Transport Properties in Back Contact Dye-Sensitized Solar Cells. *Solar Energy Mater. Sol. Energy Mater. Sol. Cells* **2009**, *93*, 720–724.
30. Reemts, J.; Kittel, A. Persistent Photoconductivity in Highly Porous ZnO Films. *J. Appl. Phys.* **2007**, *101*, 013709.
31. Sze, S. M.; Ng, K. K. *Physics of Semiconductor Devices*; John Wiley & Sons: Hoboken, NJ, 2007; pp 176−177.
32. Lien, D. H.; Hsu, W. K.; Zan, H. W.; Tai, N. H.; Tsai, C. H. Photocurrent Amplification at Carbon Nanotube-Metal Contacts. *Adv. Mater.* **2006**, *18*, 98–103.
33. Liu, P.; Sun, Q.; Zhu, F.; Liu, K.; Jiang, K.; Liu, L.; Li, Q.; Fan, S. Measuring the Work Function of Carbon Nanotubes with Thermionic Method. *Nano Lett.* **2008**, *8*, 647–651.

34. Chang, Y. H.; Liu, C. M.; Tseng, Y. C.; Chen, C.; Chen, C. C.; Cheng, H. E. Direct Probe of Heterojunction Effects Upon Photoconductive Properties of TiO_2 Nanotubes Fabricated by Atomic Layer Deposition. *Nanotechnology* **2010**, *21*, 225602.
35. Woan, K.; Pyrgiotakis, G.; Sigmund, W. Photocatalytic Carbon-Nanotube-TiO_2 Composites. *Adv. Mater.* **2009**, *21*, 2233–2239.
36. Grätzel, M. Photoelectrochemical Cells. *Nature* **2001**, *414*, 338–344.
37. Keem, K.; Kim, H.; Kim, G. T.; Lee, J. S.; Min, B.; Cho, K.; Sung, M. Y.; Kim, S. Photocurrent in ZnO Nanowires Grown from Au Electrodes. *Appl. Phys. Lett.* **2004**, *84*, 4376–4378.
38. Fan, Z.; Chang, P. C.; Lu, J. G.; Walter, E. C.; Penner, R. M.; Lin, C. H.; Lee, H. P. Photoluminescence and Polarized Photodetection of Single ZnO Nanowires. *Appl. Phys. Lett.* **2004**, *85*, 6128.
39. Li, Q. H.; Gao, T.; Wang, Y. G.; Wang, T. H. Adsorption and Desorption of Oxygen Probed from ZnO Nanowire Films by Photocurrent Measurements. *Appl. Phys. Lett.* **2005**, *86*, 123117.
40. Huang, H. M.; Chen, R. S.; Chen, H. Y.; Liu, T. W.; Kuo, C. C.; Chen, C. P.; Hsu, H. C.; Chen, L. C.; Chen, K. H.; Yang, Y. J. Photoconductivity in Single AlN Nanowires by Subband Gap Excitation. *Appl. Phys. Lett.* **2010**, *96*, 062104.
41. Liu, S.; Ye, J.; Cao, Y.; Shen, Q.; Liu, Z.; Qi, L.; Guo, X. Tunable Hybrid Photodetectors with Superhigh Responsivity. *Small* **2009**, *5*, 2371–2376.
42. Moazzami, K.; Murphy, T. E.; Phillips, J. D.; Cheung, M. C. K.; Cartwright, A. N. Sub-Bandgap Photoconductivity in ZnO Epilayers and Extraction of Trap Density Spectra. *Semicond. Sci. Technol.* **2006**, *21*, 717–723.
43. Mondal, S. P.; Ray, S. K. Enhanced Broadband Photoresponse of Ge/CdS Nanowire Radial Heterostructures. *Appl. Phys. Lett.* **2009**, *94*, 223119.
44. Zou, J.; Zhang, Q.; Huang, K.; Marzari, N. Ultraviolet Photodetectors Based on Anodic TiO_2 Nanotube Arrays. *J. Phys. Chem. C* **2010**, *114*, 10725–10729.
45. Bhattacharya, P. *Semiconductor Optoelectronic Devices*; Prentice-Hall: New York, 1997; pp 346−351.
46. Chao, Y. C.; Chen, C. Y.; Lin, C. A.; Dai, Y. A.; He, J. H. Antireflection Effect of ZnO Nanorod Arrays. *J. Mater. Chem.* **2010**, *20*, 8134–8138.
47. Chang, H. C.; Lai, K. Y.; Dai, Y. A.; Wang, H. H.; Lin, C. A.; He, J. H. Nanowire Arrays with Controlled Structure Profiles for Maximizing Optical Collection Efficiency. *Energy Environ. Sci.* **2011**, *4*, 2863–2869.
48. Cao, L.; Park, J. S.; Fan, P.; Clemens, B. M.; Brongersma, M. L. Resonant Germanium Nanoantenna Photodetectors. *Nano Lett.* **2010**, *10*, 1229–1233.
49. Cao, L.; White, J. S.; Park, J. S.; Schuller, J. A.; Clemens, B. M.; Brongersma, M. L. Engineering Light Absorption in Semiconductor Nanowire Devices. *Nat. Mater.* **2009**, *8*, 643–647.